Hindawi
Advances in High Energy Physics
Volume 2022, Article ID 4299254, 17 pages
https://doi.org/10.1155/2022/4299254

Research Article

Studying Same-Sign Top Pair Production through Top-Higgs FCNC Interactions at the HL-LHC

O. M. Ozsimsek,[1] **V. Ari**,[2] **and O. Cakir**[2]

[1]*Hacettepe University, Institute of Science, Beytepe, 06800 Ankara, Turkey*
[2]*Department of Physics, Ankara University, 06100 Ankara, Turkey*

Correspondence should be addressed to O. M. Ozsimsek; ozmusoz@gmail.com

Received 7 February 2022; Revised 24 October 2022; Accepted 2 November 2022; Published 25 November 2022

Academic Editor: Mariana Frank

We investigate the potential of the HL-LHC for discovering new physics effects via the same-sign top pair signatures. We focus on the semileptonic (electron and muon) decay of the top quarks and study the reach for a simplified model approach where top quark flavor changing could occur through a neutral scalar exchange. A relatively smaller background contribution and clean signature are the advantages of the leptonic decay mode of the same-sign W bosons in the same-sign production processes of top quark pairs. Assuming the FCNC between top quark, up-type quark, and scalar boson from the new physics interactions, the branchings could be excluded of the order $O(10^{-4})$. We use angular observables of the same-sign lepton pairs and the top quark kinematics in the process which provide the possibility of separation of new physics signal from the SM backgrounds using machine-learning techniques. We find that the same-sign top quark pair production is quite capable of testing the top-Higgs FCNCs at the HL-LHC.

1. Introduction

Among all fundamental fermions in the standard model (SM), top quark has the largest mass and causes the most serious hierarchy and plays an essential role in the metastability of the Higgs boson potential [1]. Top quark is also the last corner stone of the family structure of the SM with a huge mass gap with other members of quark content of the SM. It is the most sensitive particle for TeV scale physics in SM with Higgs boson, therefore researching the interactions of top quark is a crucial part of BSM physics.

The flavor-changing neutral currents (FCNCs) among the up or down sector quarks are not present at leading-order in both Yukawa and gauge interactions within the standard model (SM) framework. However, extremely small FCNC couplings could be generated from loop-level diagrams, which are strongly suppressed due to the Glashow-Iliopoulos-Maiani (GIM) mechanism [2]; and it is one of the unique characteristics of the SM. Besides, it sets a new horizon for new researches.

The essence and importance of GIM mechanism's veto and studying FCNC interactions lies in the decision of dropping or keeping the FCNC preventing unique feature of SM model to new physics. FCNC searches will deduce its ultimate fate without any doubt. If one can show its possibility, that would be a great progress at BSM researches.

The phenomenology of FCNC couplings has been discussed in many studies. There are scenarios including top-Higgs FCNC within supersymmetry models (including MSSM and RPV) [3–6]: the two-Higgs-doublet models (both flavor violating and conserving) [7–10], quark-singlet models [11], composite Higgs models [12], and warped extra dimensions models [13]. However, we use an effective Lagrangian formalism for top-Higgs-q (thq) FCNC interactions [14, 15] for a model-independent research and discuss our results with the expectations of present models. Then, the top quark FCNCs can also show up in the processes through the exchange of a new neutral scalar. To be specific about the branching ratio from models that are expected, we would like to summarize them at Table 1.

Table 1: Expected FCNC branching ratios from models [16].

	$t \longrightarrow$ uH	$t \longrightarrow$ cH
SM	2×10^{-17}	3×10^{-15}
QS	4.1×10^{-5}	4.1×10^{-5}
MSSM	$\leq 10^{-5}$	$\leq 10^{-5}$
2HDM (FC)	–	$\leq 10^{-5}$
2HDM (FV)	6×10^{-6}	2×10^{-3}
RPV SUSY	$\leq 10^{-9}$	$\leq 10^{-9}$

Production of two positively charged top quarks via uu $\longrightarrow$ tt resulting in an excess of same-sign lepton pairs has already been searched by the ATLAS [17]. Systematic uncertainties for the main backgrounds, including charge misidentification and fake/nonprompt leptons, are presented about 28%, 33%, and 30% for the ee, $e\mu$, and $\mu\mu$ channels, respectively. The limit on the cross section leads to a limit of $\mathrm{BR}(t \longrightarrow \mathrm{uH}) < 0.01$. Another search for flavor-changing neutral current processes in top quark decays has been presented again by the ATLAS Collaboration from proton-proton collisions at the LHC with $\sqrt{s} = 13\,\mathrm{TeV}$ [18]. The observed (expected) upper limits are set on the $t \longrightarrow cH$ branching ratio of 1.1×10^{-3} (8.3×10^{-4}) and on the $t \longrightarrow$ uH branching ratio of 1.2×10^{-3} (8.3×10^{-4}) at the 95% confidence level. A search for flavor-changing neutral currents (FCNCs) in events with the top quark and the Higgs boson is presented by the CMS collaboration [19]. The observed (expected) upper limits at 95% confidence level are set on the branching ratios of top quark FCNC decays, $\mathrm{BR}(t \longrightarrow \mathrm{uH}) < 7.9 \times 10^{-4}$ (1.1×10^{-3}) and $\mathrm{BR}(t \longrightarrow \mathrm{cH}) < 9.4 \times 10^{-4}$ (8.6×10^{-4}), assuming a single nonzero FCNC coupling. These prior works the basically constitutes the starting point of FCNC researches at post-Higgs era researches for FCNC. More recently, the limits given by CMS collaboration have been further improved as $\mathrm{BR}(t \longrightarrow \mathrm{uH}) < 1.9 \times 10^{-4} (3.1 \times 10^{-4})$ and $\mathrm{BR}(t \longrightarrow \mathrm{cH}) < 7.3 \times 10^{-4} (5.1 \times 10^{-4})$ [20].

Especially, we focus on the limits by CMS collaboration [20]; we use same effective Lagrangian up to a factor of weak coupling constant g and follow their limits on coupling constants which are 0.037 for η_u and 0.071 for η_c. In the case of ATLAS collaboration [18], they give a lower bound around 0.065 for both coupling constants. However, bear in mind that the differences mainly come from using different effective Lagrangian, which is discussed at Model Framework section. We investigate the problem by setting coupling constant 0.07 for scenarios about to introduce at following sections and try to improve the limits.

In recent years, many new collider ideas such as HL-LHC/HE-LHC/FCC [21–23] have been reported, and technical design report of HL-LHC has been published. Most promising feature of the HL-LHC collider for BSM searches is increased COM energy (14 TeV) and especially its luminosity [21] of up to $3\,\mathrm{ab}^{-1}$. Some phenomenological researches for future colliders and HL-LHC have already been started up; for tqH couplings, which have been explored at a high-luminosity $(\mathrm{ab}^{-1})ep$ colliders (with the possibility of electron beam having a polarization of 80% and electron energy being of 60 GeV), the 2σ upper limits on $\mathrm{Br}(\mathrm{t} \longrightarrow \mathrm{uH})$ have been obtained as 1.5×10^{-3} and 2.9×10^{-4} these future colliders LHeC and FCC-eh, respectively [24].

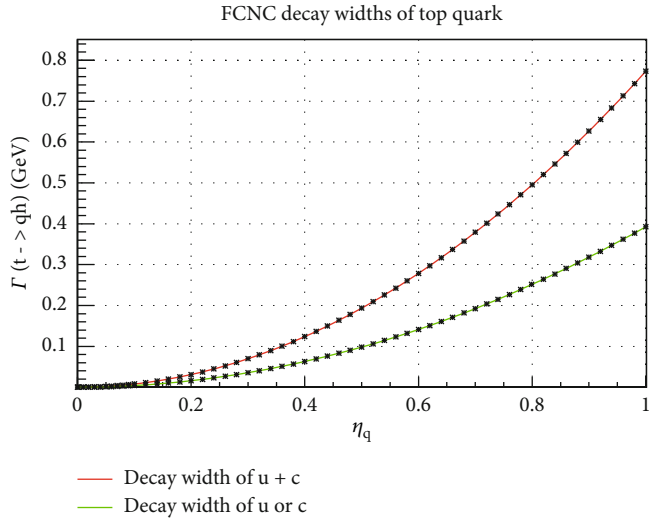

Figure 1: The FCNC decay width of top quark according to two scenarios, for $u + c$ case top quark can decay into both, otherwise decays into only one of them.

Development of such a collider has notable effects on the BSM literature evidently since it offers new possibilities for phenomenological studies and gives a large room for potential discoveries/exclusions. It offers an opportunity to rule out flavor-violating 2HDM for $t \longrightarrow$ cH case and penetrate the other regions foreseen by other models (such as Randall-Sundrum model) [25]. As a consequence, exploiting the physics potential of HL-LHC is crucial for next phase of BSM searches.

The phenomenological researches and simulations based on new colliders started to make predictions about new physics scenarios and set new limitations. To be specific at HL-LHC for FCNC interactions [26–30], branching ratios are updated as $\mathrm{BR}(t \longrightarrow \mathrm{qh}) < \mathcal{O}(10^{-4})$ using different analyses from different channels and processes; thus, couplings are expected to go below $\eta_q = 0.04$, which is roughly below the known limits from experiments. FCNC interaction projections are also available for FCC-hh. The branching ratios suggested by current phenomenological research for this collider changes at the $\mathcal{O}(10^{-6})$ and $\mathcal{O}(10^{-5})$ [31]. Expected FCNC decay widths and branching ratios are given at Figures 1 and 2, respectively, according to three scenarios which are important and handled separately to set limits for couplings in following sections.

In this study, we would like to investigate the problem and seek for the new limits at HL-LHC. To do so, we restrict ourselves to production mechanisms of same-sign $\mathrm{tt}(\overline{\mathrm{tt}})$

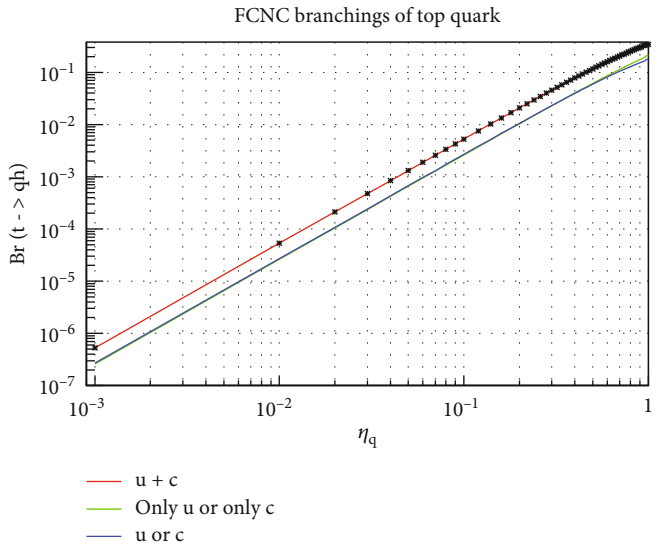

Figure 2: FCNC branchings of top quark for three scenario presented: $u + c$ indicates top quark can decay them both via Higgs. Only u or only c assumes top quark can decay only one of them and the other channel is closed. At last case, top both channels are accessible but only one of them is preferred. To access beyond the FCNC regions excluded by LHC ($\mathrm{Br}(t \longrightarrow \mathrm{qh}) \sim \mathcal{O}(10^{-3})$), one needs to set bound for the coupling constant roughly below $\eta_q = 0.04$.

pairs (signal processes $pp \longrightarrow tt \longrightarrow W^+W^+bb \longrightarrow l^+l^+bb +$ MET, $pp \longrightarrow \bar{t}\bar{t} \longrightarrow W^-W^-\bar{b}\bar{b} \longrightarrow l^-l^-\bar{b}\bar{b} +$ MET) including the exchange of Higgs boson at the HL-LHC. In addition, because the analysis was carried out in the HL-LHC, with the anticipation that the systematic uncertainties described in the literature would, in general, reduce, a value of 20% was used for the systematic uncertainties, which is still near to the limitations given in the literature and discussed in the findings section. This was done in light of the fact that the analysis was carried out in the HL-LHC. We introduce the kinematical variables to enhance the signal (S) and background (B) ratio. Angular separation of the two same-sign leptons could indicate the new physics effects in $tt(\bar{t}\bar{t})$ production process and separate the signal from background processes.

In order to make this research more detailed and similar to other studies in the literature (for comparison purposes), three different scenarios were designed for the signaling process. These are the $u + c$, only u, and only c scenarios. As the nomenclature suggests, FCNC transitions are made possible from the top quark to the other two quarks in the $u + c$ case; while in other cases, the transitions are limited to just one quark.

2. Model Framework

The flavor-changing neutral current interactions of the top quark with other particles of the SM have been described in a general way as an extension [14, 15]. This provides a direct connection between experimental observables and the new anomalous couplings. The Lagrangian describing FCNC tqH interactions in model-independent manner is given as

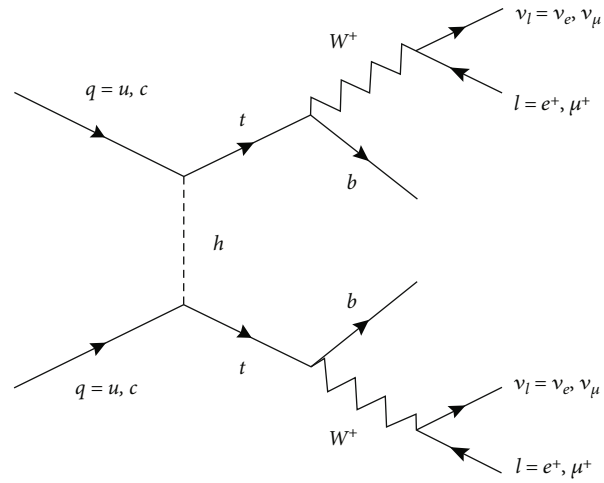

Figure 3: Feynman diagram of leptonic decay of top-Higgs FCNC process: for sake of simplicity, we give a compact form of the process which includes two new physics vertex. Dominant contribution will come from $pp \longrightarrow tt$ process due to the large values of PDF of up-type quarks in proton.

$$L_H = \frac{1}{\sqrt{2}} H\bar{t}\left(\eta_u^L P^L + \eta_u^R P^R\right) u + h.c. + \frac{1}{\sqrt{2}} H\bar{t}\left(\eta_c^L P^L + \eta_c^R P^R\right) c + h.c., \quad (1)$$

where the $\eta_q^{L/R}$ couplings set the strength of the coupling between the top quark, the Higgs boson, and up or charm quark, as well as the chirality of this coupling. They can be complex in general; however, we take into account real parts of the couplings to reduce the free parameters. In literature, this interaction can be seen as modeled without the constant

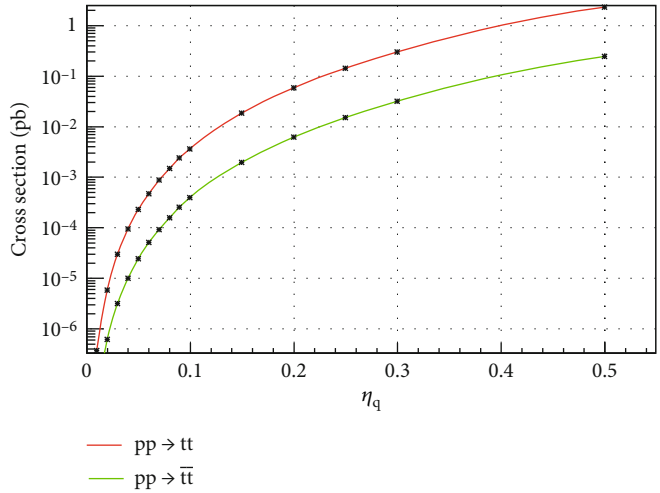

Figure 4: Estimated cross sections according to coupling constant of two same-sign lepton signal in FCNC processes. As we can see, the main contribution comes from positively charged top pair due to higher parton distributions of valance quarks at proton which differs nearly one order of magnitude. Nevertheless, adding $\overline{\text{tt}}$ production, we use negatively charged lepton pair to enhance the signal process. We assume all FCNC coefficients are the same and all channels are open (to state exactly we use $u + c \longrightarrow \eta_u = \eta_c$ case).

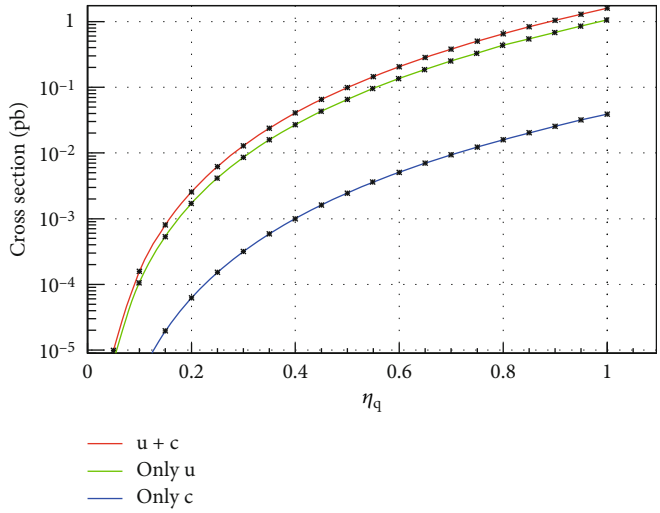

Figure 5: Cross section for the final state including two same-sign lepton at HL-LHC. Comparison of three FCNC scenarios: the matrix element of the FCNC process includes two new physics vertices which are proportional to η_q^2, hence the cross section is proportional to η_q^4. If c quark does not involve in interactions then cross section depends only on η_u^4. Since the PDF of valence u quarks are high, the contribution to cross section from u quarks are consideribly high. In the case of a forbidden u quark interaction, cross section completely depends on η_c^4 while cross section is lower. In the case of $u + c$ scenario, both u and c actively participate in interactions, there is cross term in addition to the contributions from only u and only c scenario. However, the total cross section is expected to be relatively higher than the case of only u (as shown in Figure 5), showing that the majority of interactions carry the signature of u quark distributions in the proton.

$1/\sqrt{2}$ thus gives higher top branchings a factor of 2 [32]. The FCNC processes that corresponds to tqh interactions have been described by a similar Lagrangian [19] with an extra factor of weak coupling constant. To switch between models, we just need to remind this conversion factor. We keep that constant here in order to make bounds more strict meanwhile keeping the conversion to other models in our mind. Note that it effects cross section and number of events naturally, thus it would make signal process more realistic. The decay width for FCNC channels can be calculated as

$$\Gamma(t \longrightarrow \text{qh}) = \frac{\left(\eta_{qL}^2 + \eta_{qR}^2\right)}{64\pi} \frac{\left(m_t^2 - m_h^2\right)^2}{m_t^3}, \tag{2}$$

and its numerical value depends on the coupling values

Table 2: Signal and background processes with leptonic decay channels: We consider the positively and negatively charged leptonic final states for maximal imitation of signal process. So background events generated with this regard, we force particles to give l^+/l^- final states if possible. Otherwise, we let particles to decay any channel. For W boson at intermediate states, we always take leptonic decay modes in getting the maximal similarity with signal.

Process	Cross section (pb)	Intermediate states
$pp \longrightarrow t\bar{t}(\bar{t}t)$		
$\eta_u = \eta_c = 0.07$	3.439×10^{-5}	WWbb
$\eta_u = 0.07$	5.257×10^{-4}	
$\eta_c = 0.07$	1.976×10^{-5}	
$pp \longrightarrow t\bar{t}W^{\pm}$	1.647×10^{-2}	WWWbb
$pp \longrightarrow W^{\pm}W^{\pm}jj$	1.357×10^{-2}	WWjj
$pp \longrightarrow W^+W^-Z$	1.581×10^{-3}	WWZ
$pp \longrightarrow t\bar{t}l^+l^-$	1.827×10^{-2}	WWbbll
$pp \longrightarrow ZZW^{\pm}$	1.938×10^{-4}	WZZ
$pp \longrightarrow t\bar{t}W^+W^-$	8.466×10^{-2}	WWWWbb
$pp \longrightarrow t\bar{t}Z$	1.846×10^{-4}	WWbbZ
$pp \longrightarrow ZZjj$	1.267×10^{-2}	ZZjj
$pp \longrightarrow t\bar{t}H$	4.242×10^{-5}	WWbbH

Table 3: Content of background groups: here, we grouped backgrounds to increase clarity of our histograms. The most important feature of these backgrounds are four of them includes top pair as backbone, and others only bosons. Only $pp \longrightarrow t\bar{t}l^+l^-$ process is left as own. That behavior of backgrounds leads us the categorization of them in this table.

Group name	Processes	Definition
$t\bar{t}$ w/wo boson (s)	$pp \longrightarrow t\bar{t}W^{\pm}$ $pp \longrightarrow W^+W^-t\bar{t}$ $pp \longrightarrow t\bar{t}Z$ $pp \longrightarrow t\bar{t}H$	Top pair with or without bosons or boson
Bosons w/wo jets	$pp \longrightarrow W^+W^+jj$ $pp \longrightarrow W^+W^-Z$ $pp \longrightarrow ZZW^{\pm}$ $pp \longrightarrow ZZjj$	Bosons with or without jets

Table 4: List of basic cuts.

Event selection and basic cuts
$N(\text{jets}) \geq 2$
$N(l^{\pm}) = 2$ (same sign)
$p_T^{\text{jets}} > 20\,\text{GeV}$
$p_T^{l^{\pm}} > 10\,\text{GeV}$
$\text{MET} > 20\,\text{GeV}$
$\lvert\eta^l\rvert < 2.5, \lvert\eta^j\rvert < 5$
$\Delta R(l_1, l_2) > 0.4$
$\Delta R(j_1, j_2) > 0.4$
At least one b-tagged jet

related to $\Gamma(t \longrightarrow qh) \simeq 0.1904(\eta_{qL}^2 + \eta_{qR}^2)\,\text{GeV}$. The branching ratio to an FCNC channel can be expressed as $\text{BR}(t \longrightarrow qh) = \Gamma(t \longrightarrow qh)/\Gamma(t \longrightarrow \text{all})$. Since the dominant decay mode of top quark is $\Gamma(t \longrightarrow Wb)$, this branching ratio mostly related to $(\eta_{qL}^2 + \eta_{qR}^2)$ factor especially for smaller coupling values.

The model framework can also be compared with the formalism assumed that the FCNC interactions occur via a weak sector. The relevant effective interaction Lagrangian including a new flavor-changing scalar (ϕ) is given

$$L_{\phi} = \phi\bar{t}\left(a_u + b_u\gamma^5\right)u + \phi\bar{t}\left(a_c + b_c\gamma^5\right)c + H.c., \tag{3}$$

where the coupling parameters $a_{u,c}$ and $b_{u,c}$ denote the scalar and axial couplings between top quark and up-type light

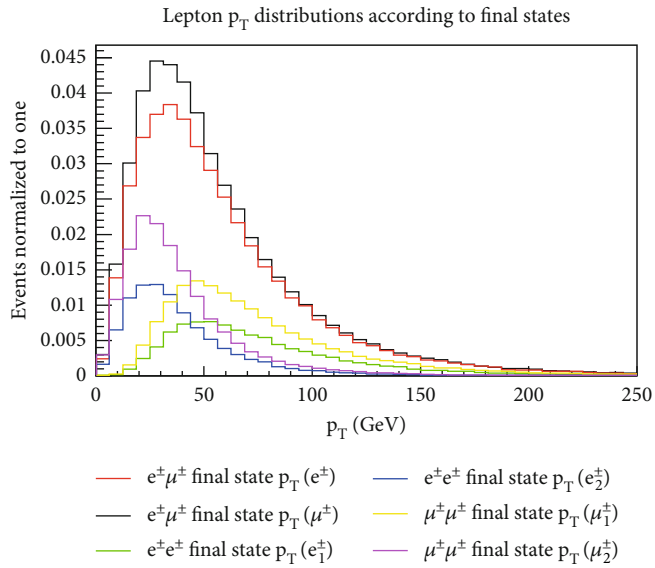

FIGURE 6: For the signal process, lepton p_T distributions $e^{\pm}e^{\pm}$, $\mu^{\pm}\mu^{\pm}$, $e^{\pm}\mu^{\pm}$ event regions: histogram clearly shows that $e^{\pm}\mu^{\pm}$ final state is more favorable. The $e^{\pm}\mu^{\pm}$ pair comes from the disintegration of $W^{\pm}$ pairs which have about 80 GeV rest mass. Hence, that energy and momentum shared by final particles give a peak around 40 GeV with boosted behavior. However, the same flavor final states shows an asymmetry originates from the following reasons: detector always discriminates lower and higher p_T particle which gives a gap between first and second highest p_T object. Nevertheless, they all have boosted behavior and give peaks close to 40 GeV as well.

quarks (u, c) which proceeds through the exchange of a scalar ϕ. To compare different formalism for the top-scalar FCNC, we find the correspondence of the couplings $a_q = (\eta_q^L + \eta_q^R)/2\sqrt{2}$ and $b_q = (\eta_q^R - \eta_q^L)/2\sqrt{2}$. Assuming no specific chirality dependence (same value for left- and right-handed couplings) of the process, we may set $a_q = \eta_q/\sqrt{2}$ and $b_q = 0$.

In this study, we use a template model. The parameters that appear in the top FCNC_UFO [33, 34] model are complex numbers in general and their real and imaginary parts can be set manually. In this work, we restrict ourselves to real parameters in order to reduce the free parameters.

3. Cross Sections of Signal and Background

At the first step before event generation, we calculate the cross section for FCNC processes including tqh, which vertices lead to same-sign signal final state as shown schematically at Figure 3. Since the cross section is proportional to the modulo quartic of the value of the anomalous couplings, in Figures 4 and 5, we can see due to presence of up-type quarks in proton, $pp \longrightarrow tt$ process is much more favorable than $pp \longrightarrow \bar{t}\bar{t}$. Although the contribution from the signal $pp \longrightarrow \bar{t}\bar{t}$ to same-sign lepton signal compared to the signal from $pp \longrightarrow tt$ is nearly less than one order of magnitude, we also use that contribution to enhance the signal.

After setting model parameters, the signal samples and background samples are generated with MadGraph5 [35]. In the partonic and hadronic level simulations, we use the parton distribution function (PDF) set NNPDF2.3 [36] at MadGraph5's default energy scale. PYTHIA 8 [37] is used for shower and hadronisation processes, and finally,

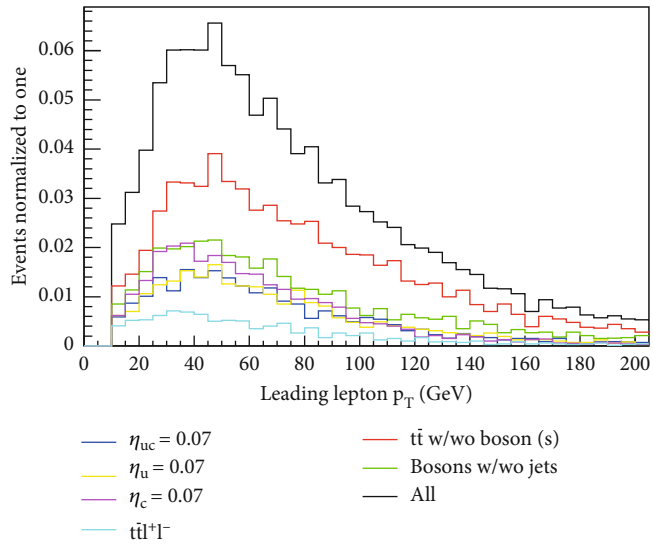

FIGURE 7: p_T distribution of signal and background processes for leading leptons.

DELPHES 3 [38] is used for detector level simulation. Result files are analyzed with ROOT6 [39].

As mentioned before, the same-sign lepton signal has relatively low background, which is advantageous and many of the background processes fall into reducible background category, which means, although they are present due to similarities between signal process, by applying proper analyze cuts, their contributions can be well reduced. However, there still exist tough irreducible backgrounds. The contributions from various backgrounds are listed below.

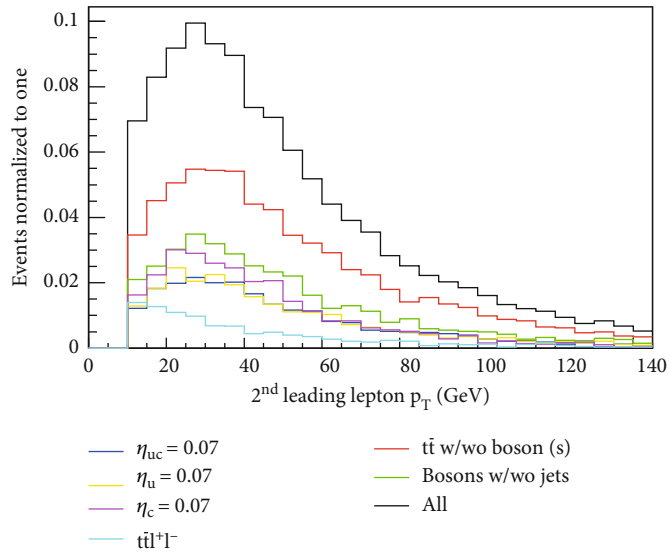

Figure 8: p_T distribution of signal and background processes for secondary leading leptons.

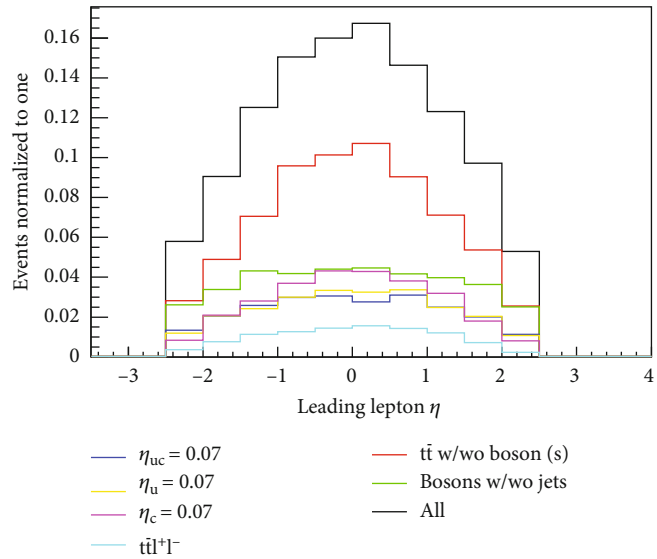

Figure 9: Lepton η distributions for signal and backgrounds: general detection is central.

Characteristics of signal events are two jets (b-tagged if possible), two same-sign leptons, and missing transverse energy. We choose our background processes by considering three fundamental features:

(i) Similarity of final state particles as much as possible with signal processes

(ii) High cross section compared to signal

(iii) Having same reconstruction inputs as for the signal

At Table 2, backgrounds have at least one of these characteristics, and several have two (at Table 3, they are grouped for simplicity). Backgrounds given in tables have at least one of these properties, besides some of them have two. As long as all processes have their own unique nature, they more or less differ at least one criterion or partly one or two criterion.

The processes $pp \longrightarrow W^{\pm}W^{\pm}jj$; $pp \longrightarrow t\bar{t}W^{\pm}$; $pp \longrightarrow t\bar{t}$ $l^{+}l^{-}$; and $pp \longrightarrow t\bar{t}W^{+}W^{-}$ with same-sign dilepton decay modes which are most similar to our signal process are directly background to our signal process and they are all irreducible. Although they give same final state content with the signal, $pp \longrightarrow t\bar{t}W^{\pm}$ reconstruction region is slightly different. This process also gives similar products at final state. However, its cross section is high. In the case $pp \longrightarrow W^{\pm}W^{\pm}jj$, on the one hand, reconstruction region is significantly different; on the other hand, its particle

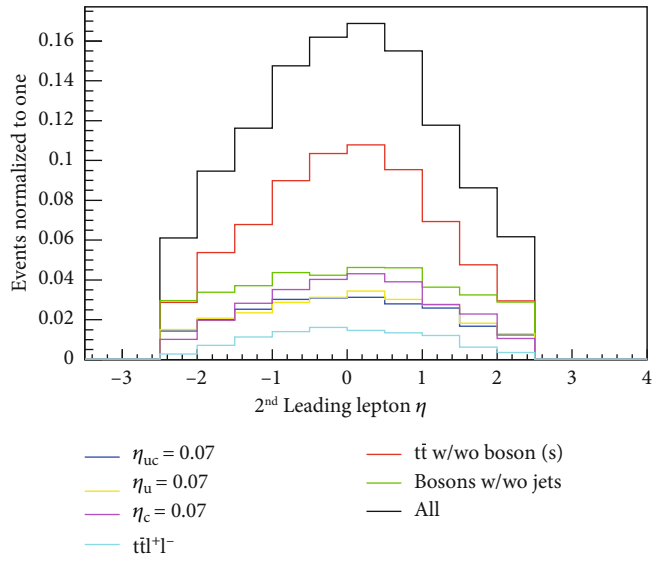

FIGURE 10: η distributions of the secondary lepton from signal and background. As can be observed, they do not form a clear cut, and their significance in the analysis is rather minor.

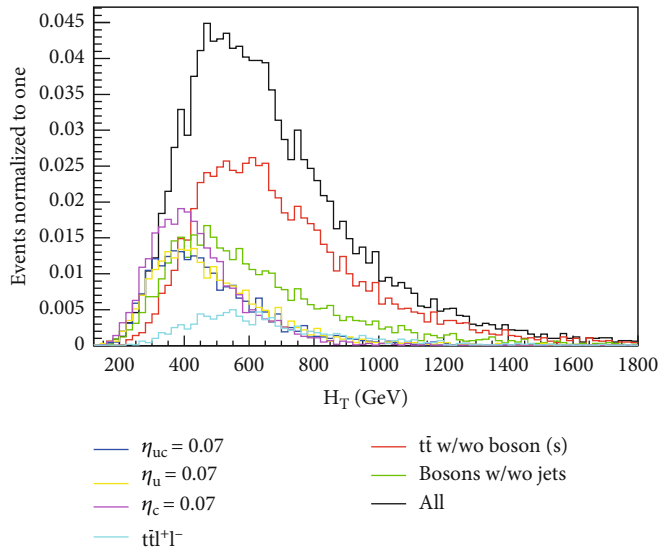

FIGURE 11: Scalar H_T distribution for the signal and background processes. Since more jet generated at backgrounds, they have relatively shifted to forward.

content is exactly the same. In addition to previous two discussions, as an advantage for analysis, $pp \longrightarrow t\bar{t}l^+l^-$ procces has low cross section compared to other two. Nevertheless, its reconstruction region is fairly same. $pp \longrightarrow t\bar{t}W^+W^-$ with leptonic decay modes directly produce signal content; however, its reconstruction region is noticeably distinct. Besides, its cross section is quite high. Similar arguments can easily be expanded to other backgrounds. Others are reducible backgrounds: even though their particle contents are similar to signal, either their cross sections are low and reconstruction region significantly different. In that regard, they satisfy only one criterion, while irreducible ones fulfill two or more.

Further, we select decay channels of background events as such to give same-sign $2l^{\pm}$ with $2j$ and MET. Jets include at least one b-tag jet. This ensures the maximum cross section for background and gives more contribution to histograms, when we consider the detector effects such as misidentification and over counting of particles.

Inability to distinguish between signal and background processes increases with misidentification of particles and loss of particles due to detector effects. These effects causes the fuzzing of characteristics of signal, while imitating the features of signal for background processes. Moreover, b-tag efficiency plays also an important role for analyzing the signal and background events since two b-tagged jets are a

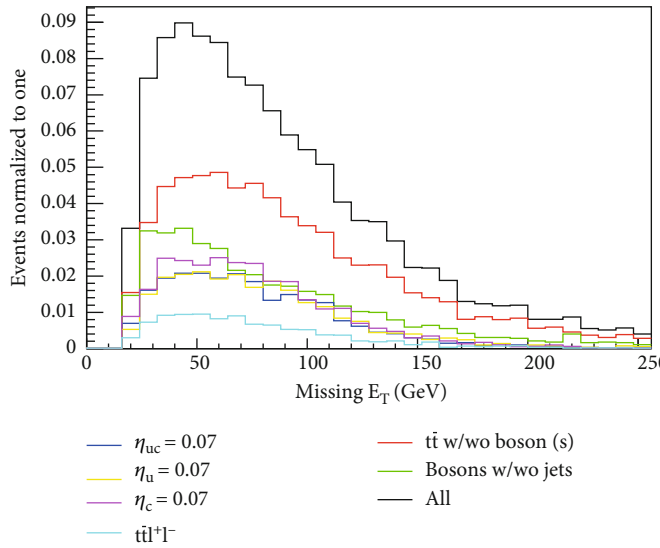

FIGURE 12: Neutrinos are the main source of missing energy of the interaction. Here, we have two neutrinos coming from $W^{\pm}$ decay. Thus, histogram gives a peak about 40-50 GeV and boosted too which are in complete consistency with our expectations.

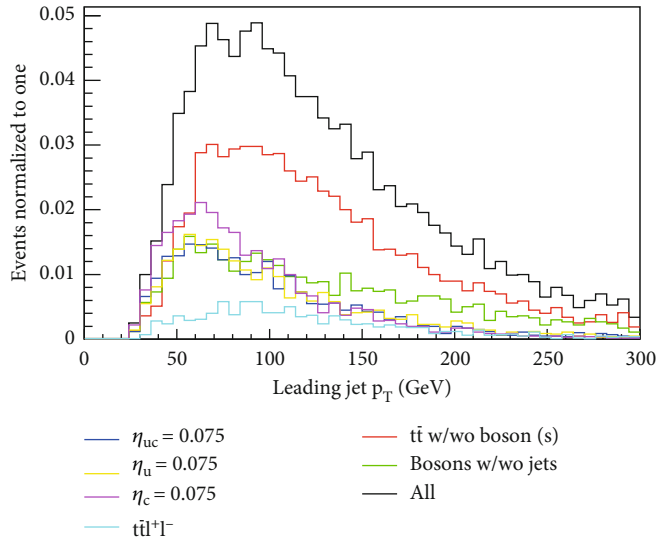

FIGURE 13: Jet p_T: even though we know our process gives mainly two b-jets, nature of process gives more jets as final state objects. Higher number of jets lowers p_T values for the jets coming from leading and second-leading jets and squeeze their p_T values below 60-70 GeV. The jets playing role at reconstructing top quarks energetic may have p_T above that values. Additionally, the effect of the longitudinal component must not be overlooked.

major property of signal. Nevertheless, two b-tagged jets requirement is so strict for observability of signal while reducing background effects too. Therefore, we confined ourselves to at least one b-tagged jet while recognizing characteristics of our signal and background processes. It is also important to note that there is no interference between signal and background at this level of calculation.

4. Analysis

At first stage, we have started with the known limits from current LHC experiments that put a limit on the FCNC coupling constant value $\eta_q = 0.07$ which is already reached; and then, use benchmark value $\eta_q = 0.07$ to insvestigate the limits for upgrading HL-LHC detector to search for a possible FCNC signal outcome. After that, we seek edge values to limit and finalize our research. We will look forward to push the limits for η_{u+c}, η_u, and η_c, separately.

We use the statistical significance SS_{disc}

$$SS_{\text{disc}} = \sqrt{2\left[(S+B)\ln\left(1+\frac{S}{B}\right)-S\right]}, \tag{4}$$

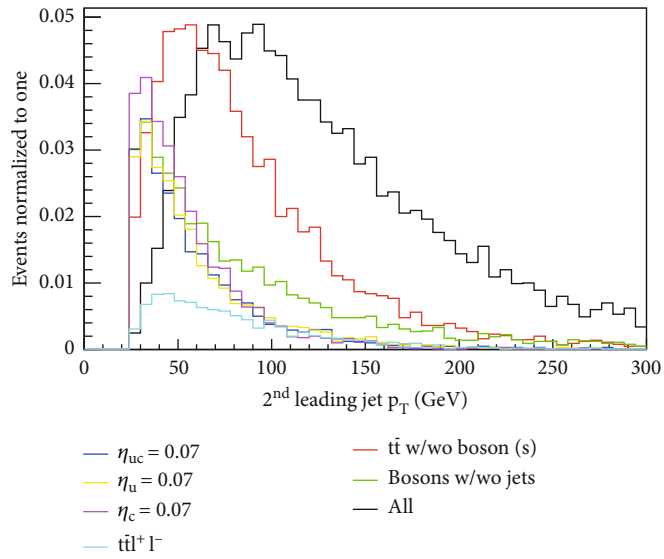

Figure 14: The overall behavior of the secondary jets in the backgrounds is highly forward, in contrast to the second jets in the signal.

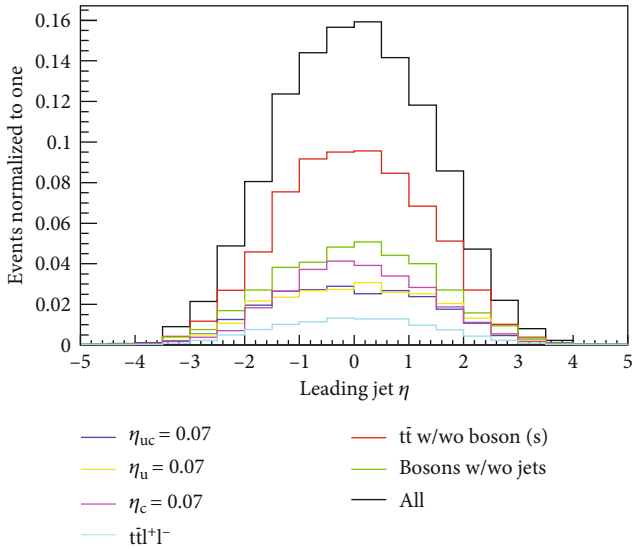

Figure 15: Leading jet η distribution at detector is central.

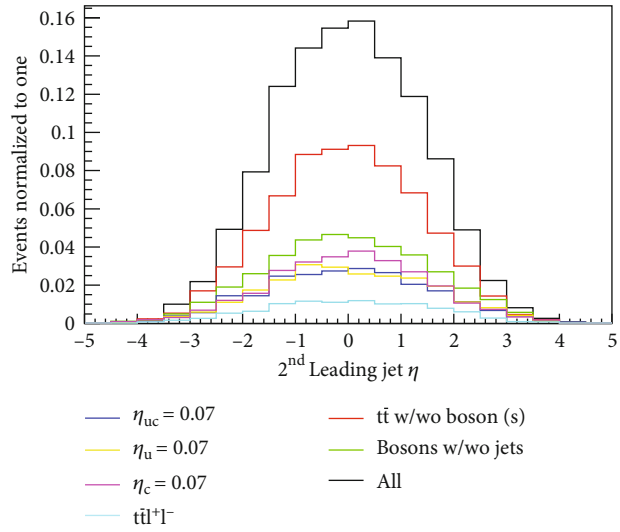

Figure 16: Second-leading jet η distribution at detector is central.

and SS_{exc}

$$SS_{exc} = \sqrt{2\left[S - B\ln\left(1 + \frac{S}{B}\right)\right]}, \tag{5}$$

for discovery and for exclusion as given in [40–43]. For the exclusion of a parameter value, we are looking for $SS_{exc} > 1.645$ corresponding to a confidence level of 95% CL. In order to make it complete, we will give limits for discovery relation too. Both relations reduce to $S/\sqrt{B}$ at large background limit. In addition, we will conduct an evaluation in which systematic uncertainties are estimated in order to comprehend how systematic uncertainties influence our results. For these calculations, we will use the following formula for discovery with systematic uncertainties

$$SSwS_{disc} = \left[2\left((S+B)\ln\left(\frac{(S+B)(B+S^2)}{B^2+(S+B)S^2}\right) - \frac{B^2}{\Delta_B^2}\ln\left(1 + \frac{\Delta_B^2 S}{B(B+\Delta_B^2)}\right)\right]^{1/2}, \tag{6}$$

and for exclusion case, we use the equation

$$SSwS_{exc} = \left[2\left\{S - B\ln\left(\frac{B+S+x}{2B}\right) - \frac{B^2}{\Delta_B^2}\ln\left(\frac{B-S-x}{2B}\right)\right\} - (B+S-x)\left(1 + \frac{B}{\Delta_B^2}\right)\right]^{1/2}, \tag{7}$$

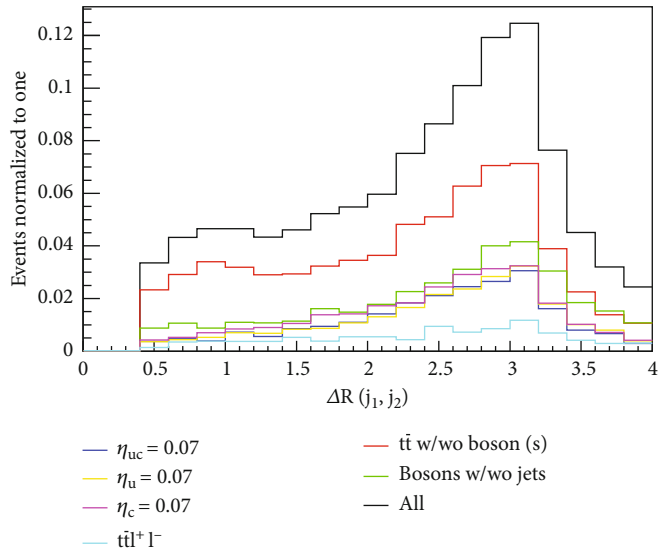

FIGURE 17: $\Delta R(j_1, j_2)$ distribution between two jets. Although there is no significant difference between the signal and background ΔR distributions at this point, it stands out as one of the most important variables since the signal process is symmetrical in its stationary frame of reference. Jets have the direct top quarks' back-to-back scattering structure.

where x being

$$x = \sqrt{(S+B)^2 - \frac{4SB\Delta_B^2}{B+\Delta_B^2}}. \tag{8}$$

When it comes to our analysis path, the first thing we'll do is focus on the key points for analysis and talk about the unique characteristics of the signaling process. These characteristics will then be disclosed by presenting the kinematic variables, and the method to be used in the study will be determined. Following that, the analysis will be performed, and the results will be provided.

Here, we will track exactly two positively/negatively charged leptons as same-sign lepton pairs since we investigate the case $W^{\pm} \longrightarrow l^{\pm}\nu_{l^{\pm}}$ followed after $t(\bar{t}) \longrightarrow W^{+}b(W^{-}\bar{b})$. Missing transverse energy is also an essential characteristics of the process too. We note that despite we have only two b-jets in our signal, when we consider the nature of interaction, more jets must be generated and we need to distinguish them from bottom quarks to reconstruct two top quarks. That point needs a little bit attention when we think of backgrounds and to make it clear, we would like to go deeper: as we know, our background events have more particles; in addition, the nature of interaction also dictates numerous jets which give more hadronic transverse energy. When we consider both, a cut that is limiting the number of jets seem to be advantageous. The best choice at first glance is limiting jet number as two, so we conclude with exact event selection. Nonetheless, taking into account detector effects, in a situation where two leptons are detected individually, if there are no jets or only one jet, these jets are more likely to escape from the detector. Working with a small number of jets is useful in this regard, as backdrops are highly prominent when working with a large number of jets. Furthermore, because the top quark is the source of leptons in the processes, it can be assumed that every case in which two same-sign leptons are seen belong to the signal event, again taking charge conservation into account. Again, b-tagging serves a purpose here. Of course, without jets, this labeling is not conceivable. However, in single-jet (or fat jet) scenarios, this criterion can be used to provide the analysis a boost.

For lepton flavors, we have 2 possibilities, namely, $e^{\pm}$ and $\mu^{\pm}$ for $l^{\pm}$ case since τ lepton disintegrates before reaching the detector, so its analysis is out of scope. In that respect, we divide the analysis region to three, which includes three possibilities of same-sign lepton pairs ($e^{\pm}e^{\pm}, \mu^{\pm}\mu^{\pm}, e^{\pm}\mu^{\pm}$) with exactly two jets, while at least one of them is b-tagged, and lastly, the presence missing transverse energy in events.

Decay of top quarks in their rest frame gives rise to high p_T b-jets larger than about 80 GeV as a prediction in addition same happens for W^{+} bosons, and daughter particles should have at least 40 GeV. These particles also carry momentum, thus we expect boosted behavior at histograms for mother and daughter particles.

To sum up at the beginning of the analysis, we have divided signal analysis into three regions with exact event selection, followed by simple cuts given in Table 4. Here, the η cuts were chosen to work with the more sensitive regions of the detector for leptons especially. Furthermore, ΔR cuts were established as the minimum lepton isolation criteria. For triggering and good object selection criteria for jets and leptons, missing transverse energy and p_T cuts are minimally incorporated. To avoid a fat-jet scenario, ΔR cut was regarded appropriate for jets, although jets reaching the detector were tolerated by avoiding an η limiting cut. As previously stated, it was noted that at least one of the jets entering the depicted histograms was b-tagged. Here, we give the kinematical distributions for lepton p_T at Figures 6–8, lepton η at Figures 9 and 10, H_T and MET at Figures 11 and 12, and lastly jet p_T and η at Figure 13–16, belonging the signal process. In addition to the variables specified, the ΔR distributions of leading jets and leptons that are

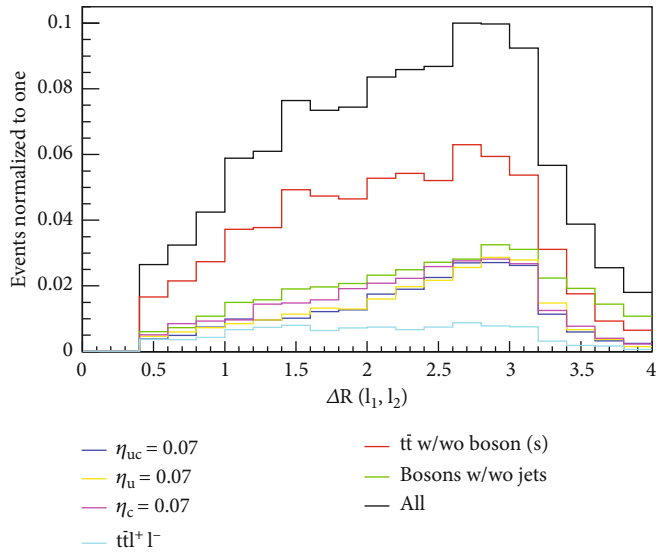

FIGURE 18: $\Delta R(l_1^+, l_2^+)$ distribution between two leptons. The ΔR variable in leptons is very crucial for discrimination, as it is in jets, but their behavior is much looser in comparison to jets due to additional energy-momentum conservation constraints from the decay of the W boson.

useful for analysis are provided at Figures 17 and 18. Finally, we present histograms showing the characteristics of jets produced and little comments on them. These histograms compare the behavior of signal and background events without delving into a detailed investigation. Except for a few cuts relevant to the study, the segments utilized for event production have been transferred to the detector level in order to provide the histograms in their simplest form, while some variables reflect differences. Although it is possible to separate the signal process, which includes two new physics vertices (and lowers cross section drastically), in the background, due to the high cross section of the $t\bar{t}W^{\pm}$ background and its similarity to the signal, it is not possible to make a discrepancy after a point and provide the desired improvement in the analysis.

Although this makes the investigated process more appealing for exclusion, because the path forward with cut-based analysis is limited, better results can be obtained by utilizing machine-learning techniques with the help of variables defined after these basic cuts.

The most fundamental variables in this analysis are the p_T, η, and ϕ components of the jets up to 4th as well as the same kinematic variables as the first two leptons. Furthermore, variables such as missing E_T, H_T, and ΔR are used together with the invariant masses of the two jets and two leptons, the invariant and transverse masses in the quadruple state (l_1, l_2, j_1, j_2), and finally $m_T^{W_{1,2}}$, $m_T^{t_{1,2}}$ reconstructions for the final state particles which are important for the result. For m_T^W and m_T^t variables, we have used the relations,

$$m_T^t = \left[\left(\sqrt{(p^l + p^b)^2 + \left|\vec{p}_T^{\,l} + \vec{p}_T^{\,b}\right|^2} + \left|\vec{p}_T^{\,\nu_l}\right| - \left|\vec{p}_T^{\,l} + \vec{p}_T^{\,b} + \vec{p}_T^{\,\nu_l}\right|^2\right)^2\right]^{1/2}, \tag{9}$$

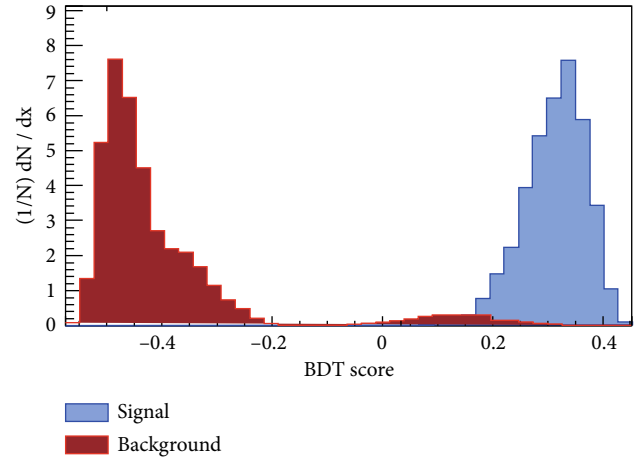

FIGURE 19: By employing an appropriate cut, it is achievable to distinguish the signal from the background with great efficiency. (The curve was determined by analyzing $\eta_{uc} = 0.07$.)

$$m_T^W = \sqrt{2p_T^l E_T^{\text{miss}} - \vec{p}_T^{\,l} \cdot \vec{p}_T^{\,\nu_l}}. \tag{10}$$

During the generation of these variables, cuts identical to those in Table 4 were utilized, with minor modifications. First, the event selection regions are separated immediately into two lepton regions with same signs, regardless of the number of jets. While the fundamental sections of the p_T cuts were kept, the criteria for lepton and jet separation were abandoned. In addition, the p_T cuts for the fifth jet remained at 15 GeV. Each η variable is set to a value less than 2.5. To contrast, the prominent signal regions in low jet number and low H_T states with the dominant background processes in high jet number and high H_T states; the number of jets is

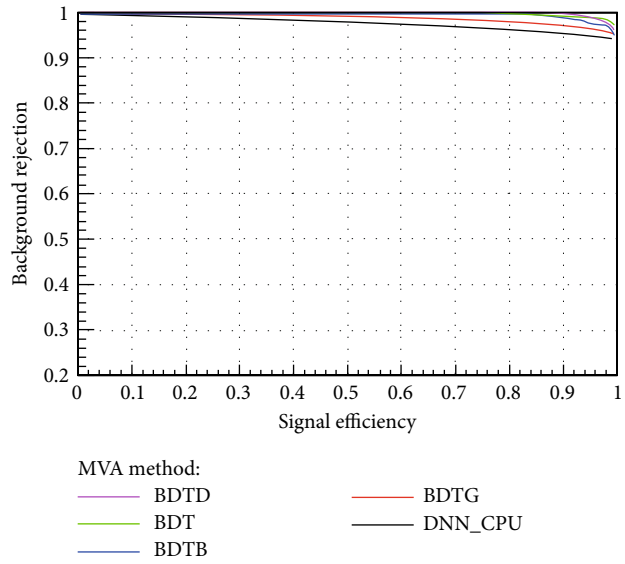

FIGURE 20: In the analysis, nonlinear approaches were predominantly employed. This is due to the fact that the structure of the signal and background distributions is more accurately reflected in this manner. In this regard, linear approaches such as Fisher's and its derivatives are unsuitable for analysis. Again, similar procedures were not adopted since they did not produce successful results. However, other nonlinear approaches were incorporated in this context so that the analysis could be compared to other ways and its evolution could be observed. The results indicate that the inputs are uniformly distributed, no overtraining was seen, and the analysis produced a high level of diversification overall.

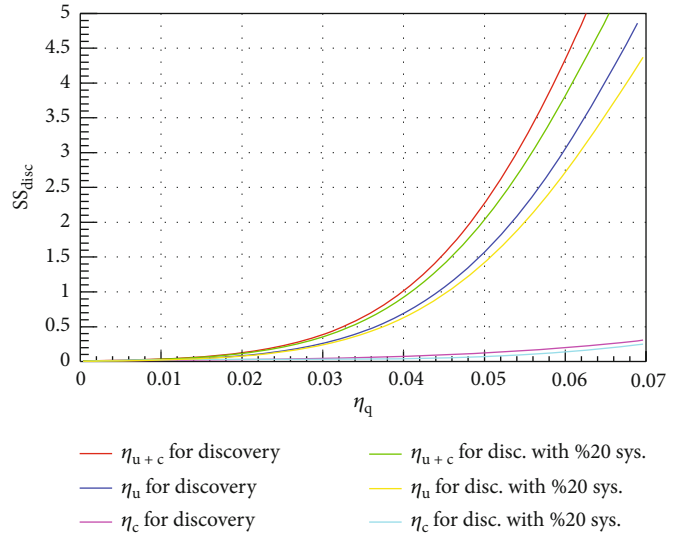

FIGURE 21: Signal significance (SS_{disc}) versus η_q-coupling parameter for three different scenarios at 3 ab^{-1}-integrated luminosity.

included up to a maximum of five and processes begin in nonjet states. In addition, the parsing of the ΔR variable was to be performed solely using machine-learning techniques [44].

Finally, the findings of the BDT analysis are presented in Figures 19 and 20. Observing the nonlinear behavior of the signal and background, suitable approaches were chosen. Since a method based on fluctuations, such as BDT, is employed. A decision tree takes a set of input features and splits input data recursively based on these features. Boosting is a method of combining many weak learnings (trees) into a strong classifier. It has been confirmed that the rate of discrimination gradually increases between the training and testing phases. Figure 19 demonstrates that, as a result of the employment of several variables with high event numbers, the distribution and height of the signal's curve are significantly superior to the back one.

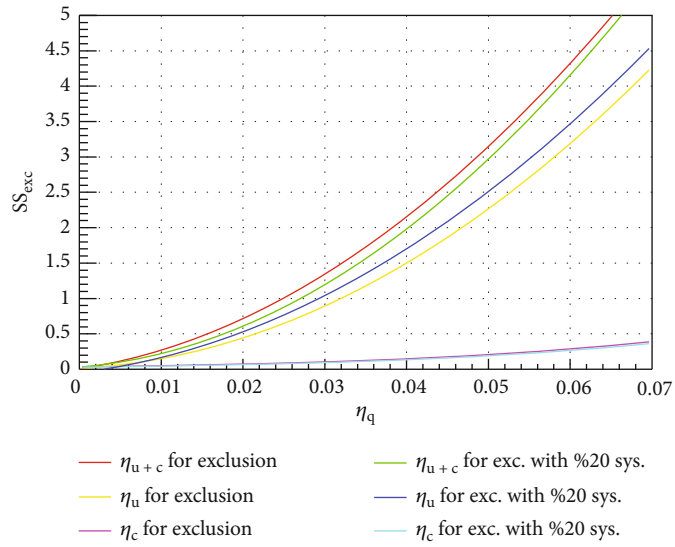

Figure 22: Signal significance (SS_{exc}) versus η_q-coupling parameter for three different scenarios at 3 ab^{-1}-integrated luminosity.

Table 5: Upper limits on η_q parameter and corresponding branching ratio as a potential discovery scenario projection at HL-LHC with no systematics (left side) and with 20% systematics (right side) at 3 ab^{-1} integrated luminosity.

Scenario	$SS_{disc} \geq 2$		20% sys.	$SS_{disc} \geq 2$	
$\eta_u = \eta_c$	0.048	0.048	$\eta_u = \eta_c$	0.050	6.52×10^{-4}
Only η_u	0.053	0.053	Only η_u	0.055	7.88×10^{-4}
Only η_c	0.12	0.12	Only η_c	0.12	3.74×10^{-3}
Scenario	$SS_{disc} \geq 3$		20% sys.	$SS_{disc} \geq 3$	
$\eta_u = \eta_c$	0.054	7.60×10^{-4}	$\eta_u = \eta_c$	0.056	8.17×10^{-4}
Only η_u	0.060	9.38×10^{-4}	Only η_u	0.062	1.00×10^{-3}
Only η_c	0.13	4.39×10^{-3}	Only η_c	0.14	5.09×10^{-3}
Scenario	$SS_{disc} \geq 5$		20% sys.	$SS_{disc} \geq 5$	
$\eta_u = \eta_c$	0.063	1.00×10^{-3}	$\eta_u = \eta_c$	0.065	1.10×10^{-3}
Only η_u	0.070	1.28×10^{-3}	Only η_u	0.073	1.39×10^{-3}
Only η_c	0.15	5.83×10^{-3}	Only η_c	0.16	6.63×10^{-3}
Scenario	$SS_{exc} \geq 1.645$		20% sys.	$SS_{exc} \geq 1.645$	
$\eta_u = \eta_c$	0.034	3.00×10^{-4}	$\eta_u = \eta_c$	0.036	3.38×10^{-4}
Only η_u	0.036	3.38×10^{-4}	Only η_u	0.040	4.17×10^{-4}
Only η_c	0.12	3.74×10^{-3}	Only η_c	0.12	3.74×10^{-3}

5. Results and Conclusions

In this study, we have searched for accessible limits for top-Higgs FCNC couplings using same-sign lepton channel at the HL-LHC (see Figures 21 and 22). This channel gives clean signal signature in addition to its low reducible/irreducible background. However, this channel suffers from two new physics vertices. Thus, these effects lower the cross section drastically which is a disadvantageous feature of this analysis. Keeping these in mind, we can conclude that simulation of this process with the same-sign lepton channel turns into a laboratory for testing the mentioned scenarios in the text. In this respect, this channel determines the upper limit for couplings and benefits exclusion limits rather than discovery.

We have started with coupling constant $\eta_q = 0.07$ to demonstrate the characteristics of signal an catch the limits given in ref. [18] whose limits are more or less same as our benchmark value. Then, as stated at introduction section, we have tried to improve our results and get better limits for FCNC couplings.

In Table 5, we summarize our analysis results with the discovery and exclusion significance. Due to the sensitivity of the study to exclusion, examining exclusion instances first will expose the results more clearly. First, the results of the initial review have improved the known limits [18–20], with the exception of some channels [20]. In addition, although how the results will be compared with one another is discussed in the second chapter, these changes will be discussed in greater detail here.

As expected, the η_{u+c} instance produced the best results. Cases η_u and η_c followed these outcomes, respectively. Theoretically and empirically, the results vary little in the idealized scenario, assuming a total of 20% systematic uncertainty. This means that the background in the study has been eliminated with great success, and these uncertainties will not significantly impact the outcomes. In the case of exclusion, we have improved the coupling constant limits for η_{u+c} and η_u situations, although our limits for η_c are more stringent. However, the branching ratios for the η_c situation appear to have already been exceeded. Similarly, the η_u and η_{u+c} scenarios exceed the LHC constraints by a small amount. At this point, as the effective Lagrangiande utilized by CMS contains a weak interaction constant, it is apparent that the results may stray further from the known limitations with this factor, despite the fact that the analysis indicates the reverse. From the obtained coupling constants, the resulting branching ratios are determined. The minimum values coupling constants attained are proportional to the number of events in the analysis, or indeed the cross section. When the analyzed process consists of two vertices, it is dependent on constants of the fourth order and has an advantage proportionate to the inverse square of the coupling constant size when compared directly. In fact, this circumstance nullifies the influence of the weak interaction constant and drastically decreases the results below the known levels. In this regard, it becomes evident why the channel is superior for exclusion and why it establishes very strict upper limits. Nonetheless, these constraints also limit other studies of top quark-Higgs FCNC interactions. Since these restrictions are precluded for this channel with two vertices, it stands to reason that studies with a single vertex will go below this limit, at least proportional to the obtained coupling constant value. Note that, we have also caught the phenomenological limits for HL-LHC expected [26–31]. At that studies η_q varies near 0.04 [27–29] (bear in mind that models does not include additional $1/\sqrt{2}$ factor and we would like to point out that some of these research focus on luminosity variation rather than limit values).

Concerning the scenario of discovery, the limits reached for discovery coincide with the limits reached by the CMS and ATLAS Collaborations at lower total luminosity values. In this instance, if further data is obtained, this value indicates that exploration is feasible up to the region's limit. However, it should not be forgotten that due to the nature of the analysis channel, they are still upper limitations. In this context, it has been proven that the values for an analysis involving a single FCNC vertex can be reduced.

Lastly, upcoming colliders will provide better visions for FCNC interactions [23]. To compare them with each other, we may say HL-LHC and FCC-eh are expected to work at same region. Moreover, HL-LHC offers better limits when we compare it with ILC/CLIC [23]. So our results have some implications on the analysis have been done for both FCC-eh and ILC/CLIC. In support of this, studies give similar results to ours done for FCC-eh [24]. Even though results of HL-LHC will give direction to new researches without any doubt, there is a gap in COM and luminosity values between HL-LHC and FCC-hh. It is expected to take down limits even further by FCC-hh. FCC-hh can possibly rule out RS models and start to penetrate the MSSM region.

To sum up our findings, we may say, while these limits are compatible with the expectations from HL-LHC, which enforce limitations for findings on other channels since on the one hand, this channel gives its clean signal fingerprint; on the other hand, even lower cross section, the same-sign lepton channel provides upper limits and provides hints to other detectors and thanks to its clean signal fingerprint, it also imposes partial limitations on other channels. Our limits can also be combined with the other sensitive channels for similar scenarios.

Data Availability

The data file used to support the findings of this study are available from the corresponding author upon request.

Conflicts of Interest

The authors declare that they have no conflicts of interest.

Acknowledgments

No funding was received for this research. The authors are grateful to Ulku Ulusoy for a careful reading of the manuscript. We wish to acknowledge the support of the AUHEP group, offering suggestions and encouragement. The numerical calculations reported in this paper were partially performed at TUBITAK ULAKBIM, High Performance and Grid Computing Center (TRUBA resources).

References

[1] D. Buttazzo, G. Degrassi, P. P. Giardino et al., "Investigating the near-criticality of the Higgs boson," *Journal of High Energy Physics*, vol. 2013, article 089, 2013.

[2] S. L. Glashow, J. Iliopoulos, and L. Maiani, "Weak interactions with lepton-hadron symmetry," *Physical Review D*, vol. 2, no. 7, pp. 1285–1292, 1970.

[3] J. Guasch and J. Solà, "FCNC top quark decays in the MSSM: a door to SUSY physics in high luminosity colliders?," *Nuclear Physics B*, vol. 562, no. 1-2, pp. 3–28, 1999.

[4] G. Eilam, A. Gemintern, T. Han, J. M. Yang, and X. Zhang, "Top-quark rare decay t -> ch in R-parity-violating SUSY," *Physics Letters B*, vol. 510, no. 1-4, pp. 227–235, 2001.

[5] J. J. Cao, G. Eilam, M. Frank et al., "Supersymmetry-induced flavor-changing neutral-current top-quark processes at the

CERN large hadron collider," *Physical Review D*, vol. 75, no. 7, article 075021, 2007.

[6] J. Cao, C. Han, L. Wu, J. M. Yang, and M. Zhang, "SUSY induced top quark FCNC decay $t \longrightarrow c\,h$ after Run I of LHC," *The European Physical Journal C*, vol. 74, no. 9, article 3058, 2014.

[7] S. Bèjar, J. Guasch, and J. Solà, "Loop induced flavor changing neutral decays of the top quark in a general two- Higgs-doublet model," *Nuclear Physics B*, vol. 600, no. 1, pp. 21–38, 2001.

[8] D. Atwood, L. Reina, and A. Soni, "Phenomenology of two Higgs doublet models with flavor-changing neutral currents," *Physical Review D*, vol. 55, no. 5, pp. 3156–3176, 1997.

[9] G. C. Branco, P. M. Ferreira, L. Lavoura, M. N. Rebelo, M. Sher, and J. P. Silva, "Theory and phenomenology of two-Higgs-doublet models," *Physics Reports*, vol. 516, no. 1-2, pp. 1–102, 2012.

[10] M. Kohda, T. Modak, and W.-S. Hou, "Searching for new scalar bosons via triple-top signature in $cg \longrightarrow tS^0 \longrightarrow t\bar{t}t$," *Physics Letters B*, vol. 776, pp. 379–384, 2018.

[11] J. A. Aguilar-Saavedra, "Effects of mixing with quark singlets," *Physical Review D*, vol. 69, no. 9, article 099901, 2004.

[12] A. Azatov, G. Panico, G. Perez, and Y. Soreq, "On the flavor structure of natural composite Higgs models & top flavor violation," *Journal of High Energy Physics*, vol. 2014, article 82, pp. 1–28, 2014.

[13] A. Azatov, M. Toharia, and L. Zhu, "Higgs mediated flavor changing neutral currents in warped extra dimensions," *Physical Review D*, vol. 80, no. 3, article 035016, 2009.

[14] J. A. Aguilar Saavedra, "Aminimal set of top anomalous couplings," *Nuclear Physics B*, vol. 812, no. 1–2, pp. 181–204, 2009.

[15] J. A. Aguilar Saavedra, "A minimal set of top-Higgs anomalous couplings," *Nuclear Physics B*, vol. 821, no. 1-2, pp. 215–227, 2009.

[16] J. A. Aguilar-Saavedra, "Top flavor-changing neutral interactions: theoretical expectations and experimental detection," *Acta Physica Pololica B*, vol. 25, pp. 2695–2710, 2004.

[17] The ATLAS Collaboration, "Analysis of events with b-jets and a pair of leptons of the same charge in pp collisions at $\sqrt{s} = 8$ TeV with the ATLAS detector," *Journal of High Energy Physics*, vol. 2015, article 150, pp. 1–51, 2015.

[18] The ATLAS Collaboration, M. Aaboud, G. Aad et al., "Search for top-quark decays t Hq with 36 fb^{-1} of pp collision data at $\sqrt{s} = 13$ TeV with the ATLAS detector," *Journal of High Energy Physics*, vol. 2019, article 123, pp. 1–67, 2019.

[19] The CMS Collaboration, "Search for flavor-changing neutral current interactions of the top quark and the Higgs boson decaying to a bottom quark-antiquark pair at $\sqrt{s} = 13\ TeV$," *Journal of High Energy Physics*, vol. 2022, no. 2, article 169, 2022.

[20] The CMS Collaboration, "Search for flavor-changing neutral current interactions of the top quark and Higgs boson in final states with two photons in proton-proton collisions at $\sqrt{s} = 13$ TeV," *Physical Review Letters*, vol. 129, article 032001, 2022.

[21] I. Bèjar Alonso, O. Brüning, P. Fessia et al., "High-luminosity large hadron collider (HL-LHC): technical design report," *CERN Yellow Reports: Monographs*, vol. 10, 2020.

[22] A. Abada, M. Abbrescia, S. S. Abdus Salam et al., "HHE-LHC: the high-energy large hadron collider," *The European Physical Journal Special Topics*, vol. 228, no. 5, pp. 1109–1382, 2019.

[23] A. Abada, M. Abbrescia, S. S. Abdus Salam et al., "FCC-hh: the hadron collider," *The European Physical Journal Special Topics*, vol. 228, no. 4, pp. 755–1107, 2019.

[24] H. Sun and X. Wang, "Exploring the anomalous top-Higgs FCNC couplings at the electron proton colliders," *The European Physical Journal C*, vol. 78, no. 4, article 281, 2018.

[25] K. Agashe, R. Erbacher, C. E. Gerber et al., "Snowmass 2013 top quark working group report," 2013, https://arxiv.org/abs/1311.2028.

[26] J. Ebadi, F. Elahi, M. Khatiri, and M. M. Najafabadi, "Same-sign top pair plusWproduction in flavor changing vector and scalar models," *Physical Review D*, vol. 98, no. 7, article 075012, 2018.

[27] Y.-J. Zhang and J.-F. Shen, "Probing anomalous *tqh* couplings via single top production in associated with the Higgs boson at the HE-LHC and FCC-hh," *The European Physical Journal C*, vol. 80, no. 9, article 811, 2020.

[28] Y.-B. Liu and Z.-J. Xiao, "Searches for the FCNC couplings from top-Higgs associated production signal with $h \longrightarrow \gamma\,\gamma$ at the LHC," *Physics Letters B*, vol. 763, pp. 458–464, 2016.

[29] Y. B. Liu and S. Moretti, "Probing the top-Higgs boson FCNC couplings via the $h \rightarrow \gamma\gamma$ channel at the HE-LHC and FCC-hh," *Physical Review D*, vol. 101, no. 7, article 075029, 2020.

[30] P. Mandrik and theFCC study group, "Prospect for top quark FCNC searches at the FCC-hh," *Journal of Physics: Conference Series*, vol. 1390, article 012044, 2019.

[31] O. M. Ozsimsek, V. Ari, and O. Cakir, "Investigating top-Higgs FCNC couplings at the FCC-hh," *Nuclear Physics B*, vol. 983, article 115908, 2022.

[32] M. Buchkremer, G. Cacciapaglia, A. Deandrea, and L. Panizzi, "Model-independent framework for searches of top partners," *Nuclear Physics B*, vol. 876, no. 2, pp. 376–417, 2013.

[33] C. Degrande, C. Duhr, B. Fuks, D. Grellscheid, O. Mattelaer, and T. Reiter, "UFO - the Universal FeynRules Output," *Computer Physics Communications*, vol. 183, no. 6, pp. 1201–1214, 2012.

[34] A. Alloul, N. D. Christensen, C. Degrande, C. Duhr, and B. Fuks, "FeynRules 2.0 – a complete toolbox for tree-level phenomenology," *Computer Physics Communications*, vol. 185, no. 8, pp. 2250–2300, 2014.

[35] J. Alwall, R. Frederix, S. Frixione et al., "The automated computation of tree-level and next-to-leading order dierential cross sections, and their matching to parton shower simulations," *Journal of High Energy Physics*, vol. 2014, article 079, 2014.

[36] NNPDF Collaboration, R. D. Ball, V. Bertone et al., "Parton distributions with LHC data," *Nuclear Physics B*, vol. 867, no. 2, pp. 244–289, 2013.

[37] T. Sjöstrand, S. Ask, J. R. Christiansen et al., "An introduction to PYTHIA 8.2," *Computer Physics Communications*, vol. 191, pp. 159–177, 2015.

[38] J. de Favereau, C. Delaere, P. Demin et al., "Delphes 3: a modular framework for fast simulation of a generic collider experiment," *Journal of High Energy Physics*, vol. 2014, article 057, 26 pages, 2014.

[39] R. Brun and F. Rademakers, "ROOT – an object oriented data analysis framework," *Nuclear instruments and methods in physics research section A: accelerators, spectrometers, detectors and associated equipment*, vol. 389, no. 1–2, pp. 81–86, 1997.

[40] G. Cowan, "Two developments in tests for discovery: use of weighted Monte Carlo events and an improved measure,"

Progress on Statistical Issues in Searches, SLAC, vol. 2012, pp. 4–6, 2012.

[41] G. Cowan, K. Cranmer, E. Gross, and O. Vitells, "Asymptotic formulae for likelihood-based tests of new physics," *The European Physical Journal C*, vol. 71, no. 2, 2011.

[42] T.-p. Li and Y.-q. Ma, "Analysis methods for results in gamma-ray astronomy," *Astrophysical Journal*, vol. 272, pp. 317–324, 1983.

[43] R. D. Cousins, J. T. Linnemann, and J. Tucker, "Evaluation of three methods for calculating statistical significance when incorporating a systematic uncertainty into a test of the background-only hypothesis for a poisson process," *Nuclear Instruments and Methods in Physics Research Section A: Accelerators, Spectrometers, Detectors and Associated Equipment*, vol. 595, no. 2, pp. 480–501, 2008.

[44] A. Hoecker, P. Speckmayer, J. Stelzer et al., "TMVA-toolkit for multivariate data analysis," 2007, https://arxiv.org/abs/physics/0703039.